

CASE STUDY

CS(AR) - 189

**SEDIMENTATION STUDIES IN MASSANJORE
RESERVOIR OF MAYURAKSHI BASIN**



जपो हिप्ता मयोमुक्

**GANGA PLAINS REGIONAL CENTRE
NATIONAL INSTITUTE OF HYDROLOGY
PATNA
1994-95**

Preface

A specific remote sensing application for turbidity measurements is in the detection and monitoring of sediment in water bodies. The presence of suspended sediment or organic materials increases the reflectance in the visible regions of the electromagnetic spectrum.

IRS-1A and IRS-1B LISS II data provide an ideal vehicle for detection & monitoring suspended sediments in large water bodies. The temporal features of these data provide a time series of the sediment concentration and its distributions. The synoptic view provided using multi-data & multi-band satellite data gives very different observations from that which can be obtained with surface data collection and sampling.

Presently, the institute has taken up a task to study changes in sedimentation and sediment distribution pattern in Massanjore reservoir of Mayurakshi river system, West Bengal, which can act as an input for state engineers, administrators and planners for detailed study of the Massanjore reservoir capacity and its water management. The Ganga Plains Regional Center, Patna after discussion with Govt. of Bihar and Govt. of West Bengal has taken up this study for Massanjore reservoir.

To study the changes in sedimentation & its distribution in the Massanjore reservoir of Mayurakshi river basin, digital image processing and visual interpretation techniques have been utilized using IRS-1B LISS II satellite (imageries and digital) data for the years 1989 and 1993. Year-wise and seasonal changes in sediment concentration in the reservoir have been analysed and delineated in maps. The results obtained are very promising and useful. These results obtained may be utilized by the planners and field engineers for hydrological analysis and better understanding of the reservoir.

This report entitled "Sedimentation studies in Massanjore reservoir of Mayurakshi basin" has been prepared by Sri Ramakar Jha, Scientist 'C' and Sri Manohar Arora, S.R.A., Regional Center, Patna under the guidance of Dr. K.K.S.Bhatia, Scientist 'F', Regional Center, Patna. Sri B.K.Sinha, Director, Bihar Remote Sensing Center and Sri S.K. Srivastava, Resource Scientist have given their technical support for the completion of the report. The support of scientific staff members namely Sri A.K.Sivadas and Sri M.B.Santhosh is appreciable.



(S.M. SETH)
DIRECTOR

TABLE OF CONTENTS

Content

Sl.no		Page
	LIST OF FIGURES	i
	LIST OF TABLES	ii
	ABSTRACT	1
1.0	INTRODUCTION	2
1.1	Remote Sensing Concept	3
1.1.1	Solar and terrestrial radiation	4
1.1.2	Atmospheric effects	6
1.1.3	Signatures	9
1.1.4	Data product generation	10
1.1.5	Data analysis	12
2.0	REVIEW	16
3.0	DIGITAL IMAGE PROCESSING	19
3.1	Image Rectification and Restoration	19
3.1.1	Geometric correction	19
3.1.2	Radiometric correction	20
3.1.3	Noise removal	21
3.2	Image Enhancement	21
3.2.1	Contrast manipulation	21
3.2.2	Spatial feature manipulation	23
3.2.3	Edge enhancement	23
3.2.4	Multi-image manipulation	24
3.2.5	Intensity-hue-saturation (IHS) Colour space transformation	25
3.3	Image Classification	25
3.3.1	Supervised classification	25
3.3.2	Unsupervised classification	25
4.0	THE RIVER MAYURAKSHI	26
4.1	The Catchment	26
4.1.1	Sub-catchment	26
4.1.2	Soil condition in the catchment	31
4.1.3	General soil profile	31
5.0	DATA COLLECTION	32
6.0	METHODOLOGY	33
6.1	Pre-field Image Interpretation	36
6.2	Ground Truth Verification	36
6.3	Post-field Work	36
7.0	RESULTS	37
8.0	CONCLUSIONS	44

LIST OF FIGURES

Sl.No	Title	Page
1.	Energy Available For Remote Sensing	5
2.	Atmospheric Windows	7
3.	Schematics Showing Radiance	8
4.	Two Dimensional Feature Space	13
5.	Index Map Of Mayurakshi River System	27
6.	Operational Capabilities Of ERDAS	34
7.	Changes In Waterspread Area	38
	1. Pre-monsoon data for the year 1989	
	2. Post-monsoon data for the year 1993	
8.	Changes In Waterspread Area	39
	1. Pre-monsoon data for the year 1993	
	2. Post-monsoon data for the year 1993	
9.	Seasonal Sediment Distribution Pattern	42
	1. Pre-monsoon data for the year 1993	
	2. Post-monsoon data for the year 1993	
10.	Yearwise Sediment Distribution Pattern	43
	1. Post-monsoon data for the year 1989	
	2. Post-monsoon data for the year 1990	

LIST OF TABLES

Sl.No	Title	Page
1.	Type of Land in the study area	28
2.	Sub-catchment areas of Mayurakshi	29
3.	Erosion prone areas of the Mayurakshi basin	30
4.	Changes in Waterspread area of the Massanjore Reservoir	40

ABSTRACT

The suspended material discharged by river into reservoir, transport pollutants and are the natural material that fill channel and reservoir. The input of suspended material to reservoir is variable in concentration and composition from river to river, as well as changing with time in any particular river. The variation in average concentration of suspended sediment in a river basin is related to seasonal changes in precipitation and run-off within the drainage basin of river. The composition of the suspended material discharge by river into reservoirs varies from river to river, depending on the composition of the rock and soils in the river drainage basin, the weather climate to which these rocks and soils have been exposed and the energy of river to transport various size of material.

Remote Sensing of reflected solar radiation can provide timely and repeated information of suspended sediment flow concentration pattern in reservoirs. Multi-temporal and multi-band satellite data are extremely useful in determining sedimentation rate in a reservoir and mapping different concentration levels of sediment load. The synoptic view provided by remote sensing gives very different data from that which can be obtained with surface data collection and sampling. In recent years, Digital image processing and visual interpretation techniques have been used to obtain the useful information on the location and extent of sediment distribution pattern in the water spread area of a reservoir.

In the present study, digital image processing and visual interpretation technique have been utilized to locate the sediment concentration in the Massanjore reservoir of Mayurakshi river basin, West Bengal-using IRS-1B LISS II satellite data. Two seasons data (pre and post monsoon) for the years 1989 and 1993 were utilized to evaluate the sediment concentration in the Massanjore reservoir. Year-wise and seasonal changes in sediment concentration at various location in the reservoir have been analyzed and delineated in a map.

1.0 INTRODUCTION

Sedimentation in reservoir is a natural phenomena. It encroaches dead storage and live storage zones of a reservoir and resulting in continuous reduction in its capacity. The decrease in storage capacity impairs the intended benefits of a reservoir.

The input of suspended sediment to reservoir is variable in concentration and composition from river to river, as well as changing with time in any particular river. The variation in average concentration is related to seasonal changes in precipitation and run-off within the drainage basin of rivers. The region of extreme seasonal variation in precipitation and run-off also have the widest variation in suspended sediment concentration and region having reasonably steady climate have the least variation in suspended sediment concentration. The effect of man on the increase of suspended sediment concentration and discharge of river has been striking. The cutting of forest planing for farmland and the multiplicity of construction project associated with man's industrial and residential expansion have markedly increased the concentration and discharge of suspended sediment. The composition of the suspended sediment discharged by rivers into reservoirs varies from river to river, depending on the composition of the rocks and soils in the river's drainage basin, the weathering climate to which these rocks and soils have been exposed and the energy of river to transport various sizes of material.

The total surface water resources of India have been assessed at 180 Mham. Of this amount only about 67 Mham is considered utilized. The present utilization of surface water is estimated to be about 30.4 Mham i.e. about 45% of total utilized surface water through existing, under construction and proposed reservoirs. Considering the inflow of sediments into the reservoir, adequate provision is made during the design phase for the storage of these sediments within the reservoir. However, problem arises when sedimentation rate exceeds the design rate and sediment gets deposited in live storage also. In Indian reservoirs whereas as design rate varies from 0.29 to 4.29 ha m/100 sq. km/year, the observed range of actual sedimentation rate is 2.19 to 23.59 ha m/ 100 sq.km/year on an average capacity annually.

The large sized sediment entering the reservoir are deposited near the mouth of the entering stream. These particles are trapped within the reservoir with nearly 100% efficiency. The finer sized sediments, clays, silts, and organic debris, remain in suspension and become mixed with the reservoir water.

The successful management of large reservoirs will be enhanced if information concerning the suspended sediment budget of the reservoirs is current and available at all times. Decision regarding reservoir management would be aided greatly if a relatively cheap, efficient and accurate means were available for determining the instantaneous suspended sediment load in large bodies of water on a continuing basis.

Remote sensing of reflected solar radiation can provide timely and repeated information concerning suspended sediment flow patterns in reservoirs. Besides monitoring of the concentration of suspended sediments, the surface area of the impoundment may easily be determined by remote sensing.

1.1 Remote Sensing Concept

Remote sensing is a multi-disciplinary activity which deals with inventory, monitoring and assessment of natural resources through the analysis of data obtained by observation from a remote platform. In other words, Remote Sensing is the science of deriving information about an object measurements made at a distance from the object without actually coming in contact with it. The observations are synoptic, provide coverage of large areas and the data is quantifiable.

In the context, any force field - gravity, magnetic or electromagnetic could be used for remote sensing, covering various disciplines from astronomy to laboratory testing of materials. However, currently the term remote sensing is used more commonly to denote identification of earth features by detecting the characteristic electromagnetic radiation that is reflected/emitted by the earth surface. Every object reflects/scatters a portion of the electromagnetic energy incident on it depending upon its physical properties. In addition objects emit radiation depending on their temperature and emissivity. If we study the reflectance/emittance of any object at different wavelengths, we get a reflectance/emittance pattern which is characteristic of that object, known as 'spectral signature'. Proper interpretation of the spectral signature leads to the identification of the object.

If the observation is made due to the electromagnetic radiation from the sun or due to the self emitted radiance it is called passive remote sensing. It is also possible to produce electromagnetic radiation of a specific wavelength or a band of wavelength to illuminate the terrain. The interaction of this radiance can then be studied by sensing the scattered radiance from the target. This process is called active remote sensing. The different stages in Remote Sensing are :

- i Origin of electromagnetic energy (sun, transmitter carried by the sensor)
- ii Transmission of energy from the source to the surface of the earth and its interaction with the intervening atmosphere
- iii Interaction of energy with the earth surface (reflection/absorption/transmission) or self-emission
- iv Transmission of the reflected/emitted energy to the remote sensor placed on suitable platform
- v Detection of the energy by the sensor converting into photographic image or electrical output
- vi Transmission/recording of the sensor output
- vii Preprocessing of the data for generation of data products.
- viii Collection of Ground Truth and other collateral information
- ix Data processing and interpretation

Thus, remote sensing system consists of a sensor to collect the radiation and a platform - an aircraft, balloon, rocket, satellite or even a ground-based sensor - supporting stand - on which a sensor can be mounted. The information received the sensor is suitably manipulated and transported back to the earth - may be telemetered as in the case of unmanned - spacecraft, or brought back through films, magnetic tapes, etc. as in aircraft or manned-spacecraft systems. The data are reformatted and processed on the ground to produce either photographs, or computer compatible magnetic tapes (CCT). The photographs/CCTs are interpreted visually/digitally to produce thematic maps and other resources information.

1.1.1 Solar and Terrestrial Radiation

Electromagnetic radiation spans a large spectrum of wavelengths right from very short wavelength gamma rays (10^{-10}m) to long radio waves (10^6m). In remote sensing, the most useful regions are the visible (0.4 to 0.7 micrometer), the reflected IR (0.7 to 3 micrometer), the thermal IR (3 to 5 micrometer and 8 to 14 micrometer) and the microwave regions (0.3 to 300 cm). The sun is the important source of electromagnetic radiation used in conventional optical remote sensing. The sun may be assumed to be a blackbody with surface temperature around 6000K. The sun's radiation covers ultraviolet, visible, IR and radio frequency regions and the maximum occurs around 0.55 micrometer which is in the visible region. However, the solar radiation reaching the surface of the earth is modified by the atmospheric effects as mentioned in next section. It is observed that all bodies at temperatures above zero degrees absolute emit electromagnetic radiation at different wavelengths, as per Plank's law.

$$W^* = \frac{2\pi h c^2}{5} \frac{1}{[\frac{c h}{k T} - 1]} \text{ wcm}^{-2}\text{u}^{-1}$$

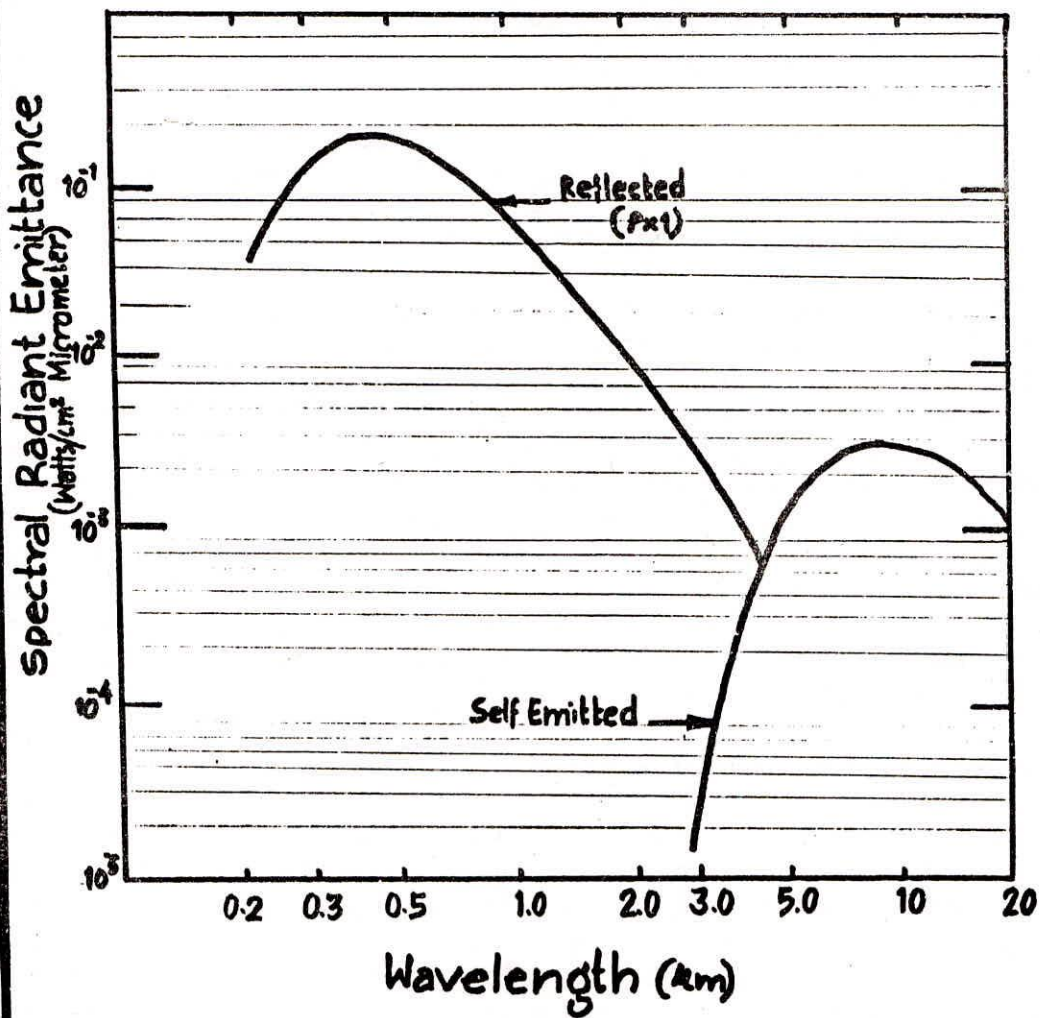


FIG. 1 : ENERGY AVAILABLE FOR REMOTE SENSING

-Atmospheric absorption not considered and
 Microwave region not shown-
 (Adapted from George Joseph and R.R Nevalgund,1991)

The earth can be treated as a blackbody at ~300K emitting electromagnetic radiation with peak emission at around 9.7 micrometer. Fig. 1 shows the spectral distribution of reflected solar self emitted thermal radiation. According to Plank's law, the radiation emitted by the earth (300 K) is much less at all wavelengths compared to the emitted by the sun (6000 K). However, at the earth's surface because of the great distance between the sun and the earth, the energy in the 7.0 to 15 micrometer wavelength region is predominantly due to the thermal emission of earth.

1.1.2 Atmospheric Effects

In passing through the atmosphere, electromagnetic radiation is scattering and absorbed by gases and particulates. Besides the major atmospheric gaseous components of molecular nitrogen and oxygen, other constituents like methane, hydrogen, helium, and nitrogen compounds play an important role in modifying the incident radiation energy spectrum. The strongest absorption occurs at wavelengths shorter than 0.3 micrometer primarily due to ozone. There are certain spectral regions where the electromagnetic radiation is passed through without much attenuation and these are called atmospheric windows (Fig.2). Remote sensing of earth's surface is generally confined to these wavelength regions. Atmospheric windows used for Remote Sensing are 0.4-1.3, 1.5-1.8, 2-2.26, 3.0-3.6, 4.2-5.0, 7.0-15.0 micrometer and 10 mm to 10 cm wavelength regions of electromagnetic spectrum. Even in the atmospheric window regions, scattering by the atmospheric constituents produces spatial redistribution of energy. Three important scattering mechanism are the Rayleigh scattering, Mie scattering and non-selective scattering.

A sensor sees the energy reflected from the target and the scattered radiation entering its field of view. The radiance measured at the top of the atmosphere has contributions from (i) single/multiple scattering of the atmospheric constituents and reaching the field of view (FOV) of the sensor (L_a), (ii) the diffused downward radiation produced by scattering which is reflected by the target of interest (L_b), (iii) the downward component reflected by an adjacent target and further scattered by the atmosphere to get into the FOV (L_c) and (iv) reflectance of the target by the direct solar radiation and attenuated to reach the top of the atmosphere - the actual information (L_T) (Fig.3). $L_a + L_b + L_c$ is usually called the path radiance. The path radiance reduces the image contrast (visually, the sharpness of the image is reduced). In addition, it produces radiometric error, since the information characteristic to target L_T is corrupted. Thus the apparent radiance of the ground targets, as measured by a remote sensor differs from the intrinsic surface

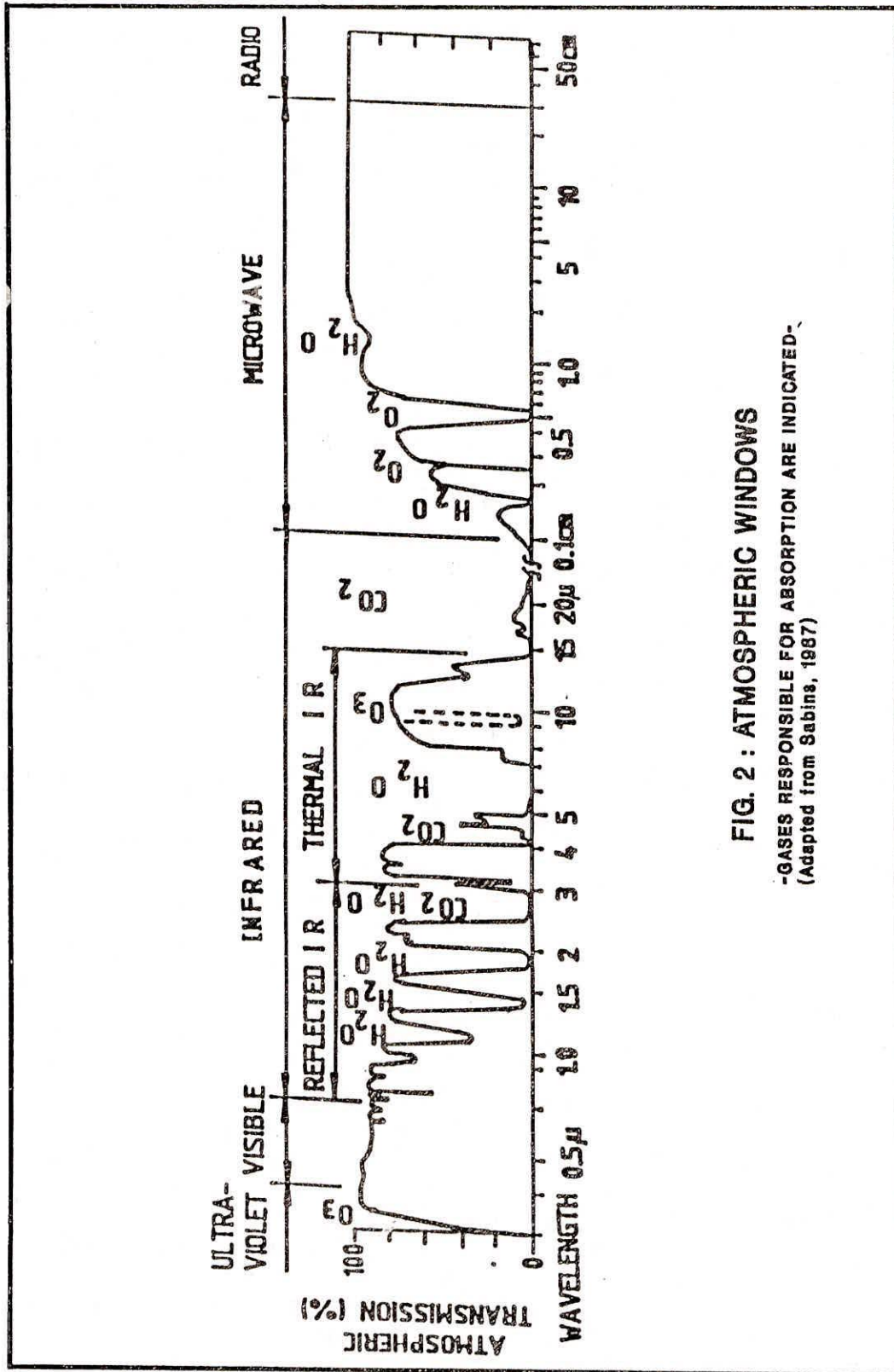


FIG. 2 : ATMOSPHERIC WINDOWS

-GASES RESPONSIBLE FOR ABSORPTION ARE INDICATED-
 (Adapted from Sabins, 1987)

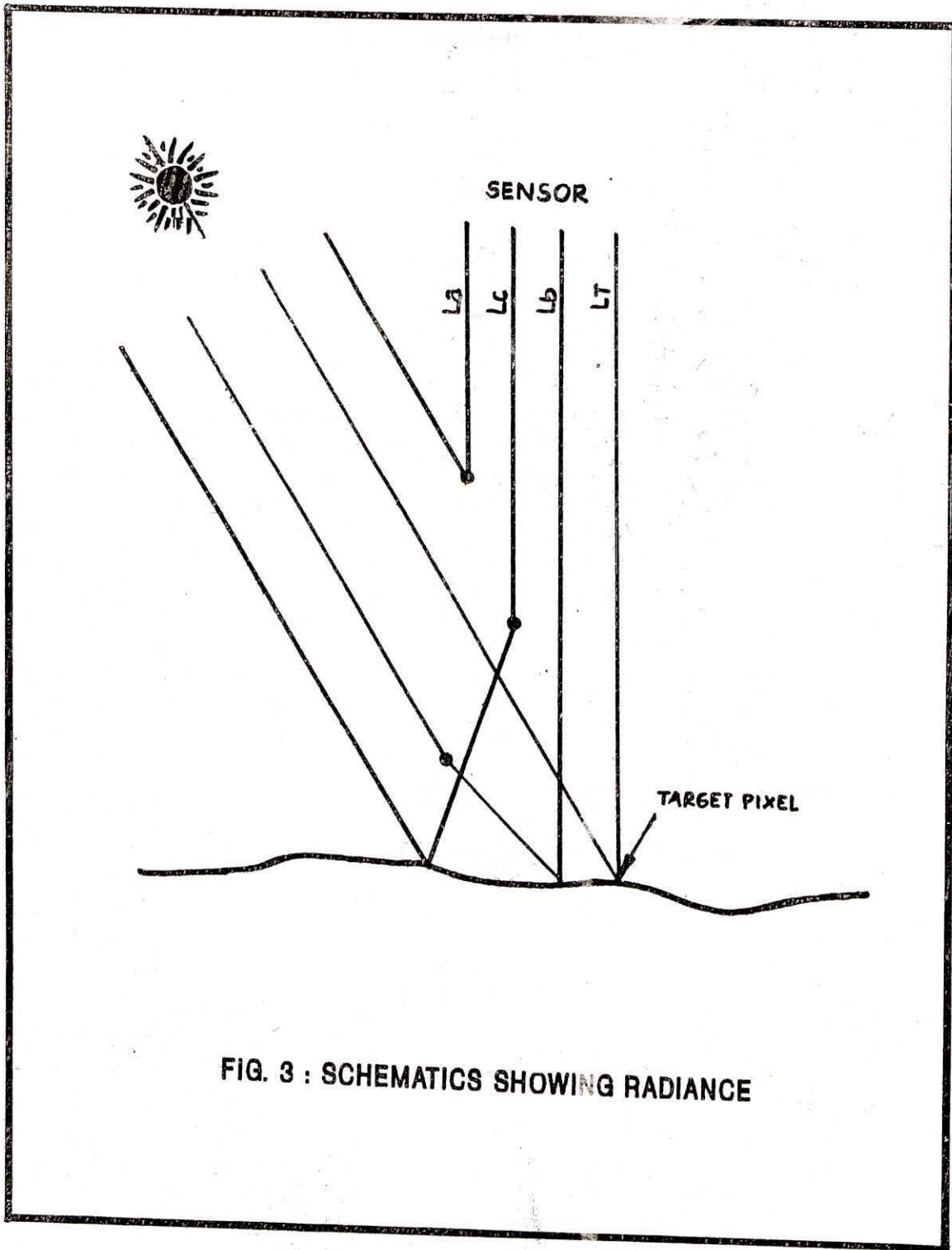


FIG. 3 : SCHEMATICS SHOWING RADIANCE

The degree of polarization is a characteristic of the object and hence can help in distinguishing the object. Such observations have been particularly useful in microwave region.

Signatures are not, however, completely deterministic. They are statistical in nature with a certain mean value and some dispersion around it.

1.1.4 Data Products Generation

The data acquired by a sensor invariably suffers from a number of errors. These errors occur due to various reasons, such as (i) imaging characteristics of the sensor, (ii) stability and orbit characteristics of the platform, (iii) scene surface characteristics, (iv) motion of the earth, and (v) atmospheric effects. Preprocessing is carried out to correct these errors to the maximum extent so that the inherent quality of the original information of the scene (such as geometry, radiometry and information content) is brought out in an optimal way. The outputs of the preprocessing, which are available in standardized formats, either in photographic or digital are known as data products.

Preprocessing is carried out for (i) eliminating geometric distortion in the imagery, (ii) eliminating radiometric distortion in the imagery, and (iii) enhancing the contrast in the data so that certain features of interest come out better in the photograph. Normally, standard data products in digital form are generated by applying geometric and radiometric corrections only, leaving the enhancement to application scientists.

The procedures employed for geometric correction generally treat distortions in two groups, viz. those which are systematic (or predictable) and those which are essentially random. Systematic errors are corrected by applying formulae derived by mathematical modelling of the expected distortions. A typical example of systematic distortions is the correction required for earth rotation. Earth rotation correction is applied on line scan image (for optomechanical and LISS type of sensors). The satellite images the earth in its south bound pass in the case of descending node acquisition. The image is made up of individual scan lines and since the earth is rotating from west to east, each successive scan line has thus to be displaced westward to correct for the relative motion between the satellite and the earth. The effect of not applying this correction is to skew the image. Other systematic distortions include the earth curvature, deviations from nominal altitude and attitude, variation of the above deviations during the imaging of a scene, etc. Random errors arise from the uncertainty in the measurement/estimation of these parameters and modelling limitations. Geometric

distortions, if left uncorrected, result in relative positional errors in latitude and longitude. To a first approximation, these distortions can be corrected from the measured/estimated parameters leaving the random errors uncorrected. The correction process proceeds by first defining the transformation equations, which relate the corrected image coordinates to the uncorrected data, using different error models and measured system parameters. The transformation equations are then applied to a selected grid of points over the scene. For the remaining point interpolation is carried out. As the transformation results in fractional scan line/pixel values in the uncorrected data, a resampling procedure is adopted to determine the gray values at these locations.

Radiometric distortion arises due to nonlinearity of the detector response, responsivity variation between the detectors, radiation pattern of antenna line and pixel drop outs. Correction factors for sensors related to radiometric errors are normally generated by extensive calibration measurements during laboratory tests. When inflight calibration techniques are employed, such information is also used for correcting post launch sensor degradation, if any. When more than one detector is used for a band, which is usually the case (6 detectors for Landsat MSS, 2048 detector elements for IRS LISS CCDs), and if the response of the detectors is not normalized by radiometric correction, one finds stripes on the image.

Image enhancement is a radiometric transformation on the pixel to enhance visual discrimination of low contrast image features. For this, the first step is to generate an image histogram, which describes statistical distribution of gray levels in an image in terms of the number of pixels comprising each gray level. One simple way to increase contrast is to expand the original gray level to fill the total dynamic range of the recording/display system. This may be achieved by subtracting a bias gray value and then increasing the gray level range with a gain factor, or by 'saturating' the lower and upper extreme of the gray values and expanding the middle range. There are a number of other linear/non-linear transformation techniques. Such enhancements are useful only for visual analysis and generally there is no advantage for digital classification.

Standard data products are generated from the corrected and formatted data by photowriting to produce photographic products in the form of black-and-white or colour transparencies or prints of different bands or combination of bands. Enlargements are generated to provide images at a specific usable scale. Digital information is provided in specific formats in computer compatible tapes. The products generated will have other auxiliary information required for data interpretation, such as

longitude and latitude mark, sun azimuth and elevation, date of acquisition and other relevant sensor related information.

1.1.5 Data Analysis

The two major methods of data analysis for extracting resource-related information from data products, either independently or in some combination with other collateral information, are visual interpretation and digital processing techniques.

A. Visual analysis

Traditionally, visual interpretation methods have been followed for extracting information on various natural resources. Tone/colour, texture, shadow, shape, size, etc. and their association are some of the basic image characteristics on which visual interpretation is based. Some of the advantages of this approach are (i) familiarity of the users with aerial photo-interpretation, (ii) images depicting the scene as though one is observing the area from a point at high altitude, and (iii) the display of spatial relations among surface features in the same context as in maps. However, visual interpretation techniques suffer from some shortcomings. The range of gray values recorded on a film or print is limited; the number of colour tones recognized by the human brain is quite large but still limited. The interpreter is likely to be subjective in discerning subtle differences in tones. It is difficult to be quantitative. It is also difficult to achieve precise registration of multi-band and multi-temporal images.

B. Digital techniques

In digital classification the computer analyses the spectral signature so as to associate each pixel with a particular feature of imagery. The reflectance value measured by a sensor for the same feature, say wheat field, will not be identical for all pixels; such response variation within a class is to be expected for any field, will not be identical for all pixels; Therefore, the radiance value for a class will have a mean and a variance. Fig.4 shows a two dimensional plot of radiance in two wavelengths for three classes, viz., for wheat, mustard and corn. This is called feature space. If we use 'n' spectral bands we get 'n' dimensional feature space. One finds a natural clustering of classes in three groups indicating the signature differences. When the cluster corresponding to different ground covers are distinct, it is easy to associated localized regions of the feature space with specific ground covers. However, such distinct clustering does not always happen in real life situations, and there could be some data set, which is not as obvious as other

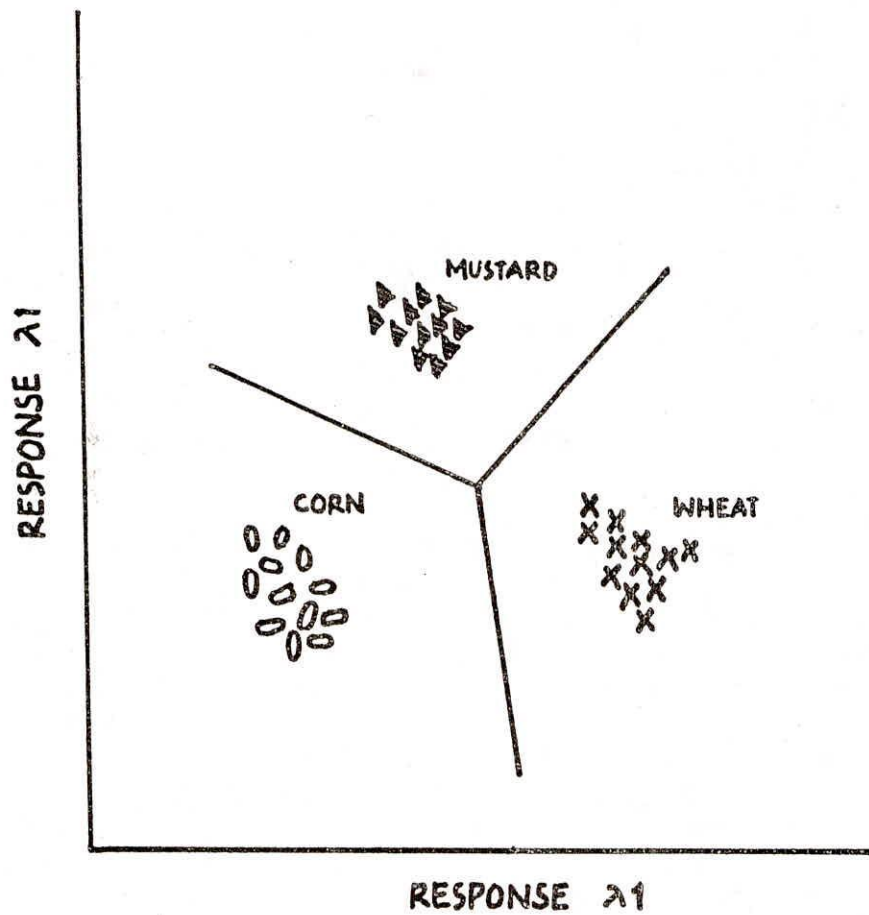


FIG. 4 : TWO DIMENTIONAL FEATURE, SPACE

(Adapted from George Joseph and R.R Navalgund,1991)

about which class it belongs. The digital classification technique essentially partitions this feature space in some fashion so that each pixel in the feature space can be uniquely associated with one of the classes. The decision to classify a pixel into any particular class from a set of data, as mentioned earlier, is statistically intelligent 'guess', which has some associated probability of error. Several classification algorithms have been developed in an attempt to minimize this error (Swain and Davis, 1978).

The digital classification techniques used can be broadly categorized into (i) supervised classifier, and (ii) unsupervised classifier. In supervised classification, the analyst locates specific sites in the remotely sensed data (based on field work, analysis of aerial data, etc.) that represent homogenous examples of various classes (like agriculture, forest, waterbody, etc.). These areas are termed as 'training sites' because the spectral characteristics of these known areas are used to 'train' the classification algorithm. For each training site, the statistical parameters like mean, variance-co-variance matrix, etc. are generated, which are used in any one of number of different classification algorithms to decide which category an unknown pixel belongs to. Each pixel is then labeled "unclassified" if it is not similar to any category. If the training sites are not properly selected, the number of misclassified/unclassified pixel increases. An output image data set is then generated using the category label assigned to each pixel. Thus, the multidimensional input image is used to develop a corresponding classified image of interpreted category types.

In contrast to this procedure, unsupervised classification is based on the exploitation of the inherent tendency of different classes to form separate spectral clusters in the feature space. Unsupervised classification uses a algorithms that search for natural groupings of the spectral properties of the pixels. The computer selects the class means and co-variance matrix to be used in the classification. Once the data is classified into cluster each cluster is then associated with a physical category.

One of the computationally simple classifier is the minimum distance to means classification algorithm. Here the analyst provides the mean vectors in each class using the training sites. Each unknown pixel with a feature vector 'X' is assigned to that class whose mean vector is close to 'x'. The distance to each mean vector from each known pixel can be calculated using Euclidean distance. This technique though simple, has poor accuracy especially when the variances of the features are quite different and large.

Gaussian Maximum Likelihood (MXL) is one of the more commonly used supervised classifiers. Basic assumption made in this case is that the training data of any class is normally distributed. Under this assumption, the distribution of gray values of given category can be completely described by the mean vector and the covariance matrix. Statistical probability of any given pixel being a member of a particular category is computed using these parameters. Evaluation of the probabilities of each pixel leads to assigning it to the class that has the maximum probability value. The pixel is said to be unclassified if the probability value are all below a threshold set by the analyst. The maximum likelihood classifier is computation intensive, since probability of a pixel belonging to each of the defined categories has to be computed.

In the present study the above said visual interpretation and digital image processing have been used to compute and map the temporal and seasonal variation in sediment distribution pattern in Massanjore reservoir of Mayurakshi river system.

2.0 REVIEW

In the last few years enormous amount of development in usage of remote sensing techniques in the fields of natural resources such as, Geology, Agriculture, Forestry, Hydrology, Land use etc. have taken place in the country. Although very limited work has been done in the water quality mapping. (Suspended sediment turbidity, salinity, chlorophyll) in river, reservoirs, lakes, estuarine system.

Water quality is an important environment variable, because it affects human health and economic activity(Alfoldi & Munday, 1978). Suspended sediment is an important environmental parameter used in determining water quality. Sediment deposition in reservoir reduces its storage capacity and hence, its ability to control flooding. Suspended matter reduces the penetration of light into water, this further reducing the production of food for fish. The poor visibility in turbid water also makes it difficult for fish to find what food is available (McCauley, 1977).

In the last few years work has been done in water quality mapping in reservoirs and lakes in India(Sahai et al, 1987; Palria et al, 1987; and Murthy et al, 1988). Muley et al (1986) visually interpreted multirate, multiband Landsat images of Wular, Dal, Chilka Lake and Rihand reservoir and indicated that band 1 and 2 give better information about turbidity levels present in the water column. Studies have shown that quantitative relationship exists between suspended sediment concentration and reflected solar radiation(Weishlatt et al, 1973; Yarger et al, 1974; Khorram et al, 1985; Ritchie et al, 1988; and Choubey, 1990).

In recent years investigators Bukata et al (1983), Khorram and Cheshire(1985), Ritchie and Cooper(1988), Lindell(1985) and Ramsay & Jensen(1990). These investigators used multi-spectral digital data and concurrently acquired field measurements to develop a predictive equation for water quality parameters. Such methods are specific by their very nature, site, and even season(Manu and Robertson, 1990). However, there still exists a need to study physical and optical properties of suspended sediments to enhance the utility of remote sensing for water quality monitoring.

Many investigators have used remote sensing techniques for water quality mapping Landsat and skylab MSS imagery and conventional aerial photographs have been used for detecting water pollution plumes and mapping sediment distribution pattern (Strandberg 1966; Klooster and Scherz 1973; Scarpate et al. 1974;

Sherz et al. 1975; Klemas et al. 1976). A number of studies have shown correlation between remotely sensed MSS data and water quality parameters such as suspended solid, secchi disk extinction depth, Jackson turbidity unit for inland waters and estuarine system (Yarger et al. 1974; Bressette 1974; Kritikos et al. 1974; Klemas et al. 1974; Bressette 1974; Kritikos et al. 1974; Klemas et al. 1974; Brooks 1975; Lilles and eta aal. 1975; Roger et al. 1974; Roger et al. 1975; Johnson 1975; Johnson et. al 1977; Johnson & Haris 1980).

Landsat and aircraft MSS digital data have been used for water quality mapping of inland and estuaries system by many investigators (Scherz et al., 1975) and utilized multispectral data to study the distributions of pollutant and algae in ocean and inland water. Landsat multispectral scanner data have been used to map concentration of suspended sediment (Klemas, 1973; Williamson and Grabeau, 1973; Johnson et. al., 1975, Rogers et. al., 1975; Ritchie, 1976, Johnson, 1978) applied regression techniques to calibrate landsat data and map distributions of chlorophyll and other water quality parameters. The same techniques have been used to map turbidity and total suspended solids (Yarger et. al 1973; Kritikos et. al 1974) Brooks, 1975; Khorram 1981, Curren et al. 1987; Rimmer 1987). Landsat data have also been used to map salinity, turbidity, chlorophyll, suspended sediment in estuarine system (Khorram 1982, 1985). The chromaticity technique have been outlined by Alfoldi & Munday (1978) and application involving suspended sediment reported by Amos and Alfoldi (1979), Munday, Alfoldi and Amos (1979) and Duffus and Press (1981), Carpenter (1983), Bukata et. al (1983), Lindell (1986).

Several investigators have studied the applicability of landsat data in determining & monitoring water quality in reservoir, lakes and estuarine system (McKeon and Rogers 1976; Rogers et. al 1975; Johnson and Harriss 1980)

Nimbus 7 - Coastal Zone Color Scanner (CZCS) was designed to detect chlorophyll, suspended solid and gelbestoffe in combinations and concentrations typical of near shore and coastal waters on continental shelf. Hovis and Leung (1977) showed that a good correlation exists between suspended sediment concentration and measured upwelling radiance recorded by the CZCS. Their results, derived using simple band ratio, discriminated SSC to approximately 100 mgL^{-1} . Thus they concluded that the CZCS could be used for quantitative interpretation of water quality. It therefore appeared likely that the sensor would discriminate inorganic suspended particulate matters in an estuarine system, large reservoirs, where levels of suspended sediment concentration is high. More accurate models for chlorophyll and turbidity concentration have been developed using ocean color

scanner data (Khorram 1981) because of narrower wavelength range.

Deekshatulu (1981), ST Chori et. al (1983), used aircraft and landsat MSS data for Hussainsagar lake and Godavari river water quality mapping. Muralikrishna (1983) and S.R. Nayak (1983) analyzed landsat data ground Gulf of cambay for sediment mapping. Study on spectral signature of water bodies with different turbidity has been done by Deekshatulu and under controlled condition by Muley. et al (1986).

For years water quality has been based on point sampling and interpolation techniques. The large size of reservoir, estuaries and the spatial variability of water quality parameters has limited the effectiveness of these techniques. From the view point of measuring water quality using landsat, considerable work has not been done in India. Therefore there is a need to investigate the usefulness of landsat data for mapping of water quality parameter primarily suspended sediment, turbidity and determining environment impact on land use practices in the basin.

3.0 DIGITAL IMAGE PROCESSING

Digital Image processing involves the manipulation and interpretation of digital images with the aid of a computer. The central idea behind Digital Image Processing is quite simple. The Digital image is fed into a Computer one pixel at a time. The computer is programmed to insert these data into an equation or series of equations and then store the results of the computation for each pixel. These results form a new digital image that may be displayed or recorded in the pictorial format.

Four broad types of Computer assisted operations for digital image processing are:

- I. Image rectification and restoration
- II. Image enhancement
- III. Image classification
- IV. Data merging

3.1. Image Rectification and Restoration

The intent of image rectification and restoration is to correct image data for distortions or degradations which stem from the image acquisition process. Image rectification and restoration procedures are often termed Preprocessing operation because they normally proceed further manipulation and analysis of the image data to extract specific information.

3.1.1 Geometric correction

Raw digital images usually contain geometric distortions such as panoramic distortions, Earth's curvature, atmospheric refraction, relief displacement and non line-writes in the sweep of a sensor's IFOV. The intent of geometric correction is to compensate for the distortions introduced by these factors so that the corrected image will have the geometric integrity of a map.

The Geometric correction process is normally implemented as a two step procedure. First, these distortions that are systematic or predictable, secondly, those distortions that are essentially random or unpredictable. Systematic distortions are well understood and easily corrected by applying formulas derived by modeling the sources of the distortions mathematically. For example, a highly systematic source of distortions are involved in Multispectral scanning from Satellite altitude in the eastward rotation of the Earth beneath the satellite during imaging. This causes each optical sweep of the scanner to cover an area slightly to the west of the previous

sweep. This is known as skew distortion. In the process of skewing the resulting imagery involves offsetting each successive scan line slightly to the west. The skewed-parallelogram appearance of satellite multispectral scanner data is a result of the correction.

Random distortion and residual unknown systematic distortions are corrected by analyzing well distributed Ground Control Points (GCP) occurring in an image. G.C.P.'s are features of known ground location that can be accurately located on the digital imagery. We first define an un-distorted output matrix of empty map cells and then fill in each cell with the gray level of the corresponding pixel or pixels in the distorted image. After producing the transformation function a process called Resampling is used to determine the pixel values to fill into the output matrix from the original image matrix.

The coordinates of each element in the undistorted output matrix are transformed to determine their corresponding location in the original input matrix.

A cell in the output matrix will not directly overlay a pixel in the input matrix. The intensity value or Digital Number (DN) eventually assigned to a cell in the output matrix is determined on the basis of the pixel values which surround its transformed position in the original input matrix.

A number of different resampling schemes can be used to assign the appropriate D.N. to an output cell or pixel. They are as follows:

- Nearest neighbor
- Bilinear interpolation
- Cubic convolution

Resampling procedures are used extensively to register image data & other source of data in GIS.

3.1.2. Radiometric correction

Is applied to any given digital image data set varies widely among sensors. The radiance measured by any given system over a given object is influenced by such factors as changes in scene illumination, atmospheric conditions, viewing geometry and instrument response.

In the case of Satellite sensing in the visible and near infrared portion of the spectrum, it is often desirable to generate mosaics in images at different times or to study the changes in the reflectance of ground features at different times

of location.

The atmosphere affects the radiance measured at any point in the scene in two contradictory ways. First, it alternates the (reduces) energy illuminating ground object. Secondly, it acts as a reflector itself, adding a scattered, extraneous path Radiance' to the signal detected by a sensor.

3.1.3. Noise removal

Is any unwanted disturbances in image data that is due to limitation in the sensing signal digitization or data recording process. The potential source of noise range from periodic drift or malfunction of a detector to electronics interference between sensor components to intermittent 'Hiccups' in the data transmission and recording sequence. Noise can either degrade or totally mark the time radiometric information content of a digital image.

The objective is to restore an image to as close an approximation of the original scene as possible. The nature of noise correction required in any given situation depends upon whether the noise is systematic, random or some combination of the two. For example, multispectral scanners that sweep multiple scan lines simultaneously often produce data containing systematic stripping or banding.

Random noise problems in digital data are handled quite differently. This type of noise is characterized by nonsystematic variation in gray levels from pixel to pixel called Bit Errors. Such noise is often referred to as being 'Spikey' in character and it causes images to have a salt and Pepper or 'Snowy' appearance.

3.2. Image Enhancement

The goal of image enhancement is to prove the visual interpretability of an image by increasing the apparent distinction between the features in the scene. Most enhancement techniques may be categorized as either Point or Local Operations.

Point Operations modify the brightness value of each pixel in an image data set independently. Local Operations modify the value of each pixel based on neighboring brightness values. The resulting images may also be recorded or displayed in black and white or in colour.

3.2.1. Contrast manipulation

Gray level thresholding is used to segment an input image into two classes - one for those pixels having values below an

analyst defined gray level and one for those above this value.

A. Level slicing

Is an enhancement technique whereby the DN's distributed along the axis of an image histogram are divided into a series of analyst specified intervals in the input image are 'slices'. All of the DN's falling within a given interval in the input image are then displayed at a simple DN in the output image. Level slicing is used extensively in the display of thermal infrared images in order to show discrete temperature ranges coded by gray level or colour.

B. Contrast stretching

Image display and recording devices typically operate over a range of 256 gray levels. Sensor data in a single image rarely extend over this entire range. The intent of contrast stretching is to expand the narrow range of brightness values typically present in an input image, over a wider range of gray values. The result is an output image that is designed to accentuate the contrast between features of interest to the image analyst. A more expressive display would result if we were to expand the range of image levels present in the scene to fill the range of display values (0-255), the range of image values has been uniformly expanded to full the total range of output device. This uniform expansion is called a Linear Stretch. The linear stretch would be applied to each pixel in the image using the algorithm.

$$DN' = \frac{(DN - MIN)}{(MAX - MIN)} \cdot 255$$

Where,

DN' = Digital Number assigned to pixel in output range.

DN = Original Digital Number of pixel in input range

MIN = Minimum value of input image to be assigned a value of 0 in the output image.

MAX = Maximum value of input image to be assigned a value of 255 in the output image.

The values for DN and DN' must be discreet whole integers. The same function is used for all pixels in the image, it is usually calculate for all possible values of DN before processing the image. The resulting values of DN' are stored in a table (array). Each pixel's DN is simply used to index a location in the table to find the appropriate DN' to be displayed in the output image. This process is referred to as a table look up procedure and the list of DN's associated with each DN is called

a look up table (LUT).

3.2.2 Spatial feature manipulation

Spatial filtering emphasize or de-emphasize image data of various spatial frequencies. Spatial frequencies refers to the roughness of the tonal variations occurring in an image.

Spatial Filtering is a 'Local' operation. In that pixel values in an original image are modified on the basis of the gray levels of neighboring pixels.

A. Lowpass filters

Are designed to emphasize low frequency features and de-emphasize the high frequency components of an image.

B. High pass filters

Do just the reverse.

Convolution

One special application of the goveric image processing operation is called Convolution. Convolving an image involves the following procedures :

1. A moving window is established which contains an array of co-efficients or weighting factors such arrays are referred to as operators or kennals and they are normally the odd number of pixels in size. (Eg. : 3 x 3, 5 x 5 etc.)
2. The kennel is moved throughout the original image and the DN at the center of the kennel is a second output image is obtained by multiplying each coefficient in the kennel by the corresponding in the original image and adding all the resulting products.

3.2.3 Edge enhancement

For many remote sensing earth science applications, the most valuable information that may be derived from an image is contained to the edges surrounding various objects or features of interest. The edge enhancement operation delineates those edges and thereby makes the shapes and details comprising the image more conspicuous and perhaps easier to analyze.

A. Linear edge enhancement

One simple method of extracting edges in remotely sensed

imagery is the application of the running difference operation. The original image is shifted by one picture element and the tested for difference between corresponding pixels in the original and shifted images.

B. Non-linear enhancement

Non-linear edge enhancement are performed using non linear combination of pixels.

3.2.4 Multi-image Manipulations

A. Spectral Ratioing

Ratio image are enhancement resulting from the division of DN values in one spectral band by the corresponding values in another band. Ratioed images are often useful for discriminating subtle spectral variations in a scene that marked by the brightness variations in images from individual spectral bands or in standard colour composites. This enhanced discrimination is due to the fact that retrieved images clearly portray the variations in the shapes of the spectral reflectance curves between the two bands involved, regardless of the absolute reflectance values observed in the bands.

B. Principal component analysis (P.C.A.)

Has proven to be a significant value in the analysis of remotely sensed digital data. The transformation of the row remote sensor data using P.C.A can result in new principal component images that are often more interpretable than the original data. P.C.A analysis may be used to compress the information content of a number of bands of imagery into just two or three transformed principal component image.

C. Vegetation component

The collection of accurate, timely information on the World's food and fiber crops continuous to be important. Kanth and Thomas derived a linear transformation of the few Landsat MSS bands that established for new axes in the spectral data that can be interpreted as vegetation components useful for agricultural crop monitoring. This 'Tassled Cap' transformation rotates the MSS data such that the majority of information is contained in two components or features which are directly related to physical scene characteristics. Brightness, the first feature, is a weighted sum of all bands and is defined in the direction of the principal variation in soil reflectance. The second feature, greenness is approximately orthogonal to brightness and is a contrast between the near-infra red and visible bands. Greenness

is strongly related to the amount of green vegetation present in the scene. Brightness and greenness together typically express 95% or more of the total variability in MSS data and here the characteristics of being readily interpretable features generally applicable from scene to scene.

3.2.5 Intensity-hue-saturation (IHS) Colour Space Transformation

Digital Images are typically displayed as additive colour composites using the three primary colours, Red, Green & Blue (RGB)

Intensity-Hue-Saturation System - 'Intensity' relates to the total brightness of a colour. 'Hue' refers to the dominant or average wavelength of light contributing to a colour. 'Saturation' specified the purity of a colour relative to gray.

3.3 Image Classification

3.3.1. Supervised Classification

The identity and location of some of the land owner types, such as urban, agriculture, wetland and forest are known a priori through a combination of field work, analysis or aerial photography, maps and personal experience. The analyst attempts to locate specific sites in the remotely sensed data that More areas are commonly referred to as Training Sites because the spectral characteristics of these known areas are used to 'train' the classification alongwith for eventual land cover mapping of the remainder of the image.

Important aspects of conducting a rigorous and useful supervised classification are:

- An appropriate classification must be adopted.
- Representation, training sites must be selected including an appreciation for signative extension factors if possible.
- Statistics must be extracted from the training site spectral data.
- The statistics are analyzed to select the appropriate features to be used in the classification process.
- Select the appropriate classification algorithm.
- Classify the imagery into one class.

3.3.2. Unsupervised classification

In an unsupervised classification the identities of land cover types to be specified as classes within a scene features within the scan are not well defined.

4.0 THE RIVER MAYURAKSHI

The Mayurakshi River has its origin on the slopes of Trikut hills about 43 km (27 miles) upstream from Dumka in Bihar (Fig.5). At its origin it is known as Matihara. In its course downwards towards the south-east, it takes in number of rivulets, streams and tributaries. The prominent among its tributaries are Bhurburi, Dhobai, Pusaro, Tepra, Bhamri, Dauna and Sidheswari. The confluence of Sidheswari with Mayurakshi is downstream of Massanjore reservoir. Tilpara Barrage on the River Mayurakshi is downstream of the confluence of these two rivers.

Mayurakshi River is 70 km (44 river miles) in length from its origin to the reservoir site out of which 43 percent (30 km) lies in the reservoir waterspread area. On this river, Mayurakshi Reservoir was created in 1954 by the construction of a stone masonry dam at Massanjore in the Santhal Parganas district of Bihar about 24 km (15 miles) from West Bengal border to irrigate the lands in West Bengal and Bihar by high level and low level canals respectively and to generate 4,000 kW hydel power. The lake extends over 30 km (19 river miles) upstream in Bihar State.

4.1 The Catchment

The 1859.62 sq. km (718 sq. miles) catchment of the river above Mayurakshi Dam is leaf shaped with no appreciable vegetal cover. Rolling and undulating in nature with scattered hillocks the catchment comprises various types of lands (Table 1).

The forests constitute only 6 percent of the catchment area. The vegetation is generally limited to hill tops and slopes. 44 percent of the catchment area comprises lands under paddy cultivation with field bunds subjects to limited soil erosion. But rest 50 percent of the catchment area is subject to sever erosion.

4.1.1 Sub-catchments

The whole catchment can be studied by dividing it into seven sub-catchments (Table 2).

From the aerial survey maps, the soil conservation Department of the Govt. of Bihar prepared the erosion interpretation maps of the catchment. From the latter the stage of erosion in each of the following catchments is inferred (Table 3).

The catchment is under various stages of erosion i.e. sheet erosion, gully erosion and ravines. Sub-catchments I and II are

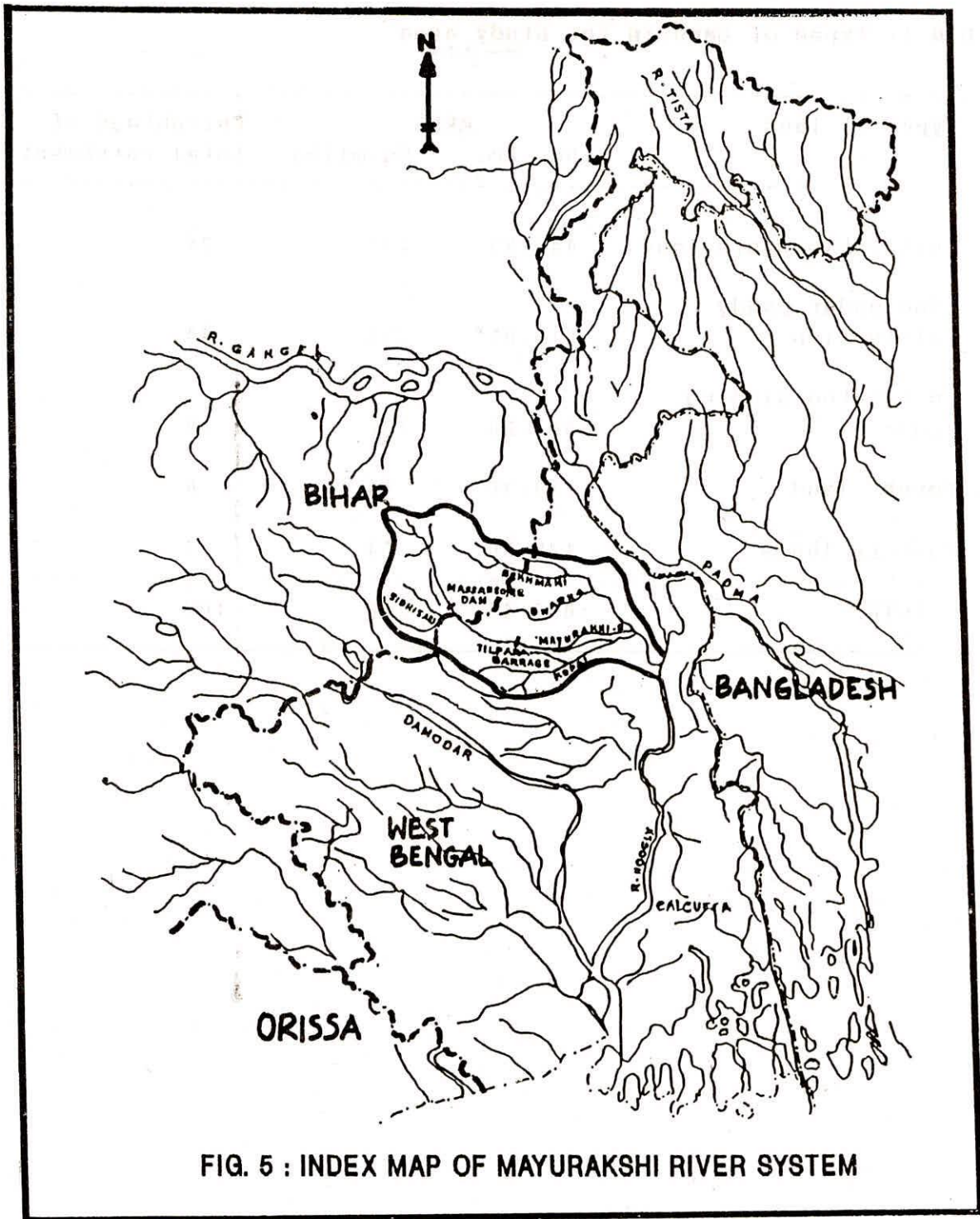


FIG. 5 : INDEX MAP OF MAYURAKSHI RIVER SYSTEM

Table 1: Types of Land in the Study area

S Types of land No.	<u>AREA</u>		Percentage of total catchment
	Sq. km.	Sq.miles	
1. Cultivable waste land	442.89	171	24
2. Land under paddy cultivation	815.85	315	44
3. Cultivated sloping lands	341.88	132	19
4. Forest land	113.96	44	6
5. Pasture lands	139.86	54	7
TOTAL	1854.44	718	100

Table 2: Sub-catchment areas of Mayurakshi basin

Sl.No.	Sub-catchment	Catchment		Percentage of total catchment
		sq. km	sq.miles	
1.	Matihara	360.01	139	19.4
2.	Dhobai	341.88	132	18.4
3.	Bhurbhuri	199.43	77	10.7
4.	Tepra	380.73	147	20.5
5.	Mayurakshi Left Bank	181.30	70	9.7
6.	Mayurakshi Right	253.82	98	13.7
7.	Dauna	142.45	55	7.6
	TOTAL	1859.62	718	100.00

TABLE 3: Erosion prone areas of the Mayurakshi basin

Sl. Sub-catchment	% of total catchment	Area in sq miles	Area under erosion: as % of sub-catchment area					Area under erosion in sq miles already in various stage of erosion
			Ravine	Gully	Sheet	Sheet	Total	
1. Matihara	19.4	139	0.096	6.640	12.700	1.010	20.446	28.5
2. Dhobai	18.4	132	0.870	4.350	7.300	10.550	23.070	30.2
3. Bhurbhuri	10.7	77	0.242	2.040	5.360	0.440	8.082	6.2
4. Tepra	20.5	147	0.284	3.820	5.260	0.286	9.45	13.9
5. Mayurakshi L.B.	9.7	70	0.468	2.570	3.440	0.784	7.262	5.2
6. Mayurakshi R.B	13.7	98	0.148	2.270	2.940	1.920	7.278	7.0
7. Dauna	7.6	55	0.146	0.814	0.930	0.844	2.734	1.5
								92.5 sq miles

1 sq mile = 2.59 sq. km

subject to maximum erosion. Out of 50 percent of the catchment area 929.81 sq. km (350 sq. miles) susceptible to heavy erosion 26 percent of it 239.58 sq. km (92.5 sq. miles) is already under various stages of erosion.

Due to indiscriminate deforestation and annual forest fires the forest area is being denuded. Excessive grazing of pasture lands has contributed to their accelerated erosion. Agricultural lands other than paddy lands with poor crop-density are continuously losing top soil. In many places gravely and rocky substrata are exposed.

4.1.2 Soil conditions in the catchment

1. Hill tops

The soils are lithosolic in nature, shallow to moderately deep with stones and gravels on the surface.

2. Foot-hills

Moderately deep to deep soils. Loose surface soil with low water retentive capacity and high susceptibility to erosion.

3. Medium Sloping Lands

Deep to very deep soils of medium to heavy texture.

4. Low-lying Lands

Soils developed from alluvial and colluvial material with high percentage of fine material.

4.1.3 General soil profile

- (i) 22.86 cm (9 in.) sandy loam, loose when dry, friable when moist.
- (ii) 22.86 cm - 5.1 cm (9 in. - 2ft) : sandy clay loam slightly hard when dry, firm when moist.
- (iii) 0.6 m - 1.2 m (2 - 4ft); sandy clay tendency to separate out as loose rocky structure on drying, firm when moist.
- (iv) 1.2 m - 1.5m (4-5ft) : strong coarse rocky structure very firm when moist but plastic when set.

The type of soils, the deteriorating conditions of the catchment due to improper land use indicate heavy erosion process in the catchment and high sediment-transport in the river down to the reservoir.

5. DATA COLLECTION

To study the temporal and spatial sediment distribution pattern in Massanjore reservoir of Mayurakshi river system, West Bengal, the following multi-date and multi-band data were utilized:

SNo.	Satellite	Sensor	Image/ Bands	Path/ Row	Date of Pass	Remarks
1.	IRS-1A	LISS II	FCC 2 3 4	19/ 51	April 6,89	For visual interpre- tation
2.	IRS-1A	LISS II	FCC 2 3 4	19/ 51	Dec. 4,89	---"---"
3.	IRS-1A	LISS II	DIGITAL 1 2 3 4	19/ 51	April 6,89	For digit- al analy- sis
4.	IRS-1A	LISS II	DIGITAL 1 2 3 4	19/ 51	Dec. 4,89	---"---"
5.	IRS-1B	LISS II	DIGITAL 1 2 3 4	19/ 51	March 17,93	---"---"
6.	IRS-1B	LISS II	DIGITAL 1 2 3 4	19/ 51	Dec. 6,93	---"---"

6. METHODOLOGY

Presence of sediment in water changes the back scattering characteristics of the water. Suspended particles tend to increase the total scatter and back scatter matter, reduce the average path length and consequently change the spectral distribution of light. Thus, a turbid water is more reflective than clear water.

Monitoring of suspended sediment concentration is an important parameter for reservoirs. Although, the sedimentation is a natural process, the rate can be accelerated or decelerated by man's activity, cutting forests, planning of farmland, construction projects, composition of rocks and soils and seasonal changes in precipitation and runoff within the drainage basin.

In the present study, visual interpretation and digital image processing techniques have been used to obtain the information on the location and extent of sediment distribution pattern in the water spread area of the Massanjore reservoir of the Mayurakshi river system, West Bengal using remote sensing data of different wavelength ranges of the electro-magnetic spectrum (bands).

In visual interpretation technique the imageries (FCC) of IRS-1A LISS II satellite data of the bands 2 (0.52-0.59 μm), 3 (0.62-0.68 μm) and 4 (0.77-0.86 μm) were obtained for the dates April 6, 1989 and December 4, 1989. The following procedure has been adopted for visual interpretation technique:

1. Some basic image characteristics such as tone, colour, texture, shadow, shape, size and their association were used to map sediment distribution pattern in the Massanjore reservoir.
2. Field survey was conducted and toposheets and other reference materials were collected to support the sediment distribution pattern obtained by imageries.
3. The water spread area of the reservoir was measured from multitemporal imageries. Seasonal changes in the water spread area and corresponding fluctuations in the sediment distribution pattern were analyzed visually.

In the digital image processing technique ERDAS (Earth Resources Data Analysis System) software has been used to carry out digital image processing and analysis of Massanjore reservoir sediment data. The ERDAS uses mathematical and logical algorithms based on Physics and Statistics to process the digital data obtainable from the satellite. The details of the operational capabilities of the ERDAS are shown in Fig. 6.

In the present study, following procedure has been adopted

ERDAS 7.5 PC Menu

<p>Core</p> <p><u>Annotation:</u> ANNOAT ANTGRID</p> <p><u>Color/Mode:</u> COLORMOD</p> <p><u>Core Image Processing:</u> CLUSTR HISTOEQ IPX LUTMOD RGBCLUS WPM</p> <p><u>Core Raster/GIS:</u> GISEDT INDEX RECODE MATRIX OVERLAY SEARCH CURVE CURVES CURBOX DIGSCRN SMEASURE</p> <p><u>Utilities:</u> CALC CONFG DIAG MSTEST CHED</p> <p><u>View:</u> BLANK CLASOVR DISPLAY DISPOL FLICKER GEOVR MOVIE READ TOGGLE ZOOMER</p> <p><u>Demos:</u> CICLE DMPSCRN PIC</p> <p><u>File Management:</u> Header/trailer: BSTATS CLASNAM CVT73 CVT74 FIXED LISTIT Create/subset: CPTSCR CUTTER MAKEPL MASK STITCH SUBSET</p>	<p>Image Processing</p> <p><u>Classification:</u> CLUSTR ISODATA MAXCLAS PPDCLAS</p> <p><u>Enhancement:</u> ALGEBRA ADIALGE DCONVLV DHISTEQ HSTMATCH LSCAN PRINCE STRETCH TEXTURE</p> <p><u>Geometric Corrections:</u> COORDN DESKEW GCP LRECTIFY NRECTIFY PROGCP</p> <p><u>Post-Classification:</u> CLASERR POLYCAT RANOCAT THRESH</p> <p><u>Pre-Classification:</u> Training Sample Selection: ISODATA SEED SIGEXT STATCL</p> <p><u>Training Sample Evaluation/Manipulation:</u> MATRIX DIVERGE ELLIPSE SIGCVRT SIGDIST SIGMAN</p> <p><u>Radioometric Corrections:</u> BADLIN DESTRIIP</p>	<p>Raster GIS Modeling</p> <p><u>AGGIE</u> CLUMP DSCASCII DSCEDIT GISMO INQUIRE POLYFIL SCAN SIEVE SUMMARY</p>	<p>Hardcopy</p> <p><u>Color/Hardcopy:</u> GISMAP LANMAP PANELMAP OCR TEKDHP</p> <p><u>Hardcopy Utilities:</u> CLRCHRT PRTCALB PRTLS SCALMAP</p>	<p>3D</p> <p>CREATED3D GEOM SEEN</p>	<p>Image Scanning</p> <p>ESCAN MAFTAC VIDDIG</p>	<p>Multivariate Image Analysis</p> <p><u>Analysis/Display:</u> BLANKIMA LOADPLOT MASKTRAN OVERSCEN OVERVIEW</p> <p><u>RESICALC</u> SCENVIEW SCORMASK SCORPLOT</p> <p><u>Preprocessing:</u> LOCMODEL PCAMODEL SCORCALC</p>	<p>Topographic</p> <p><u>Terrain Analysis:</u> RELIEF RESCALE ROTATE SLOPE</p> <p><u>Surfacing:</u> CONTOUR SORT SURFACE</p>	<p>Tapes</p> <p><u>Input:</u> AUTLOAD LOADVHR LOADATA LOADD LOADX LOADDEM PREVIEW RDASCI</p> <p><u>MTCOUNT</u></p> <p><u>Output:</u> DPDATA DUNPBIL DUNPISO WRASCI</p>	<p>Tablet Digitizing</p> <p>DIGPOL MEASURE</p>
---	---	---	--	---	---	--	---	---	---

FIG. 6 : OPERATIONAL CAPABILITIES OF ERDAS

for digital image processing using ERDAS:

1. Pre-monsoon and post-monsoon data of bands 1(0.45-0.52 μm), 2(0.52-0.59 μm), 3(0.62-0.68 μm) and 4(0.77-0.86 μm) from IRS-1A and IRS-1B LISS II were obtained for the years 1989 and 1993 and FILE MANAGEMENT option was used to make the digital data readable by ERDAS.
2. All the digital data were geometrically corrected by IMAGE PROCESSING. Image to map and image to image rectification was performed for all the digital data.
3. In order to separate land and water components, a binary mark was made by determining an interactive threshold of band 4 & the water spread area were delineated for all the scenes. Digital number(ranging from 0 to 255) of all the bands were used to differentiate water body from the land surface.
4. To study the suspended sediment concentration distribution within the Massanjore reservoir, digital data of bands 1 and 2, were utilized specifically in the analysis. The wavelength range of electro-magnetic spectrum in band 1 and 2 is reflected by the turbid water and the suspended sediment present in the water. For deep water depth also, the turbidity and presence of suspended sediment can be observed in bands 1 and 2 of the digital data. The digital numbers(ranging from 0 to 255)obtained from the satellite shows the presence of suspended sediment in the reservoir and its pattern(is0-concentration lines can be plotted).
5. The combination of bands 2, 3 and 4 was used to get the total effect of the solar radiation and to analyze the presence of suspended sediment in the water. The ENHANCEMENT and CLASSIFICATION options were used to get the sediment distribution pattern in the reservoir.
6. The analysis was carried out using several basic image analysis capabilities of ERDAS, such as histogram manipulation, histogram equalization, bstats, fixhed, subset, cutter, zoomer, overlay, linear rectification, automatic stretch display, filtering, transformation, classification, enhancement and other standard functions.
7. A maximum of five concentration level could be tried with significant variation in the reservoir using bands 2, 3 & 4.
8. Changes in water-spread area of the reservoir during the seasons and years have been analysed by OVERLAY and SUMMARY.
9. Changes in sediment concentration levels in pre-monsoon and post-monsoon seasons and also during the years 1989 through 1993 were obtained by OVERLAY and SUMMARY.
10. COLORMOD was used to give colours to all sediment concentration levels and classified as very high, high, moderate, slight to moderate and slight.
11. ANNOTAT was used for symbols, titles and sub-titles writing in the image file.

12. HARDCOPY was used to take the colour prints of the output file.

The above discussed methodology for visual interpretation and digital image processing and has been used to get the sediment distribution map of the study area and the updated map (final map) of the sediment distribution pattern in the Massanjore reservoir has been obtained by the following three phases:

1. Pre-field image interpretation
2. Ground truth verification and collection of data &
3. Post-field analysis.

6.1 Pre-field Image Interpretation

It consists of the two steps :

- (a) Preparing of base map.
- (b) Preparation of reservoir sediment concentration map.

The base map covering the Massanjore reservoir has been prepared with the help of topographic map of the study area. Some ground control points were used for transferring details into these base map.

Temporal digital image satellite data and imageries were used to assess the sediment distribution pattern in the Massanjore reservoir. ERDAS software, light table, optical enlarger and other remote sensing instruments / equipments were used for analysis. The interpretation has been done using digital numbers, tone, pattern, shape, size association and pixel gray values ranging from 0 to 255.

6.2 Ground Truth Verification

The pre-field interpretation maps were taken to the field for ground truth verification. Toposheets, field survey and other reference material available were used and carried out wherever confusion derived during interpretation.

6.3 Post-field Work

After pre-field interpretation & ground truth verification all the scenes were analyzed updating all the maps.

7. RESULTS

The distribution of suspended sediment within a reservoir depends on the volume of flood water level at the onset of the flood period and the distribution of flood water at the end of the flood period. These parameters can be measured using pre-monsoon and post-monsoon satellite data.

In the present study, the visual interpretation technique was adopted for the pre-and post monsoon imageries(FCC) of Bands 2,3 and 4 of IRS-1A LISS II data base. It gives sediment concentration levels based on their tone, texture, colour, shadow and their association. Due to limited tonal variation and limitation in visual interpretation of the imageries three sediment concentration levels could be obtained. Significant changes in sediment concentration in pre-monsoon and post-monsoon imageries has been observed and mapped.

The digital image processing technique was used to get further detailed information and precise observation of sediment distribution pattern in Massanjore reservoir. Due to high potential & capability of computer programmes much more informations of sediment distribution pattern could be obtained and analyzed by digital image processing using ERDAS software. The digital data of each band (wavelength regions of electromagnetic spectrum) 1,2,3 and 4 were used separately and also, in combination to get precise and updated sediment distribution pattern in the waterspread area of the reservoir. Each pixel of the digital data represents a gray value (reflected Electro Magnetic Radiations) between 0 to 255 based on the nature, water quality, sedimentation & turbidity of water in the reservoir. These gray values of each band has been used in the present study for pre-monsoon and post-monsoon data for the years 1989 and 1993 of IRS-LISS II satellite to compute and analyze:

1. waterspread area and changes in waterspread area in the reservoir during the seasons and years
2. The sediment distribution pattern & changes in temporal sediment distribution pattern in the reservoir.

The waterspread area of pre- and post-monsoon seasons for the years 1989 and 1993 are illustrated in Fig.7 and Fig.8 . The waterspread area in the year 1993 has increased drastically as compared to the waterspread area of the year 1989 which indicates the sediment deposition in the reservoir during this period. Also, the changes in waterspread area in both pre-and post-monsoon seasons data of the years 1989 and 1993 has been observed and mapped(Table 4).



1. PRE-MONSOON DATA FOR THE YEAR 1989.



2. POST-MONSOON DATA FOR THE YEAR 1989.

FIG. 7 : CHANGES IN WATERSPREAD AREA



1. PRE-MONSOON DATA FOR THE YEAR 1993.



2. POST-MONSOON DATA FOR THE YEAR 1993.

FIG. 8 : CHANGES IN WATERSPREAD AREA

Table 4 : Changes in Water Spread Area of the Massanjore Reservoir

Sl. No.	Date	Water Level at Dam	Water Spread Area Computed		% Change Increase
			Initially by Curve	By Remote Sensing Digital Data	
1.	Dec.4, 1989	117.7m	54.2 sq.km.	59.125 sq.km.	0.09
2.	Mar., 1993	112.59m	35.30 sq.km.	36.825 sq.km.	0.043
3.	Dec., 1993	119.7m	61.40 sq.km.	68.50 sq.km.	0.114

The sediment distribution pattern in the reservoir obtained using ERDAS software are shown in Figs. 9 and 10. The sediment concentration levels in the reservoir have been classified into a maximum of five classes. The classes of sediment concentrations levels can be increased depending on the level of information to be extracted and precision of work. Fig. 9 shows, the changes in sediment distribution pattern in pre-and post-monsoon seasons whereas Fig.10 illustrates the variation in sediment distribution pattern in post-monsoon season during the years 1989 and 1993. These figures indicates the following features:

1. In turbid water, the reflectance of EMR is observed to be higher at low wavelength bands 1 (0.45-0.52 μm) and 2(0.52-0.59 μm).
2. The sediment concentration is high along the tail end and at the river inflow area of the reservoir. This is because of arrival of sediments from flood water through the main channel in the reservoir.
3. The remote sensing techniques finds it difficult to analyze the sediment concentrations in deep water. Therefore, the deep water area i.e. near the reservoir axis (spillway) shows no turbidity. But in the pre-monsoon seasons data the sediment concentration levels could be identified due to shallow water depth. It indicates that the sediment concentration is minimum at reservoir axis which indicates sediment deposition in the bed at reservoir axis. Band 1 and 2 data gives better information of sediment distribution pattern upto 20 m deep water. Deeper water do not show any sediment distribution pattern and indicates no sediment concentration.
4. The Figs.9 and 10 illustrates significant increase in high and moderate sediment concentration level areas during the period from 1989 to 1993. The area of very little or no sediment concentrations is decreasing from year 1989 to 1993. It shows that the area near the reservoir axis is being affected by suspended sediments.

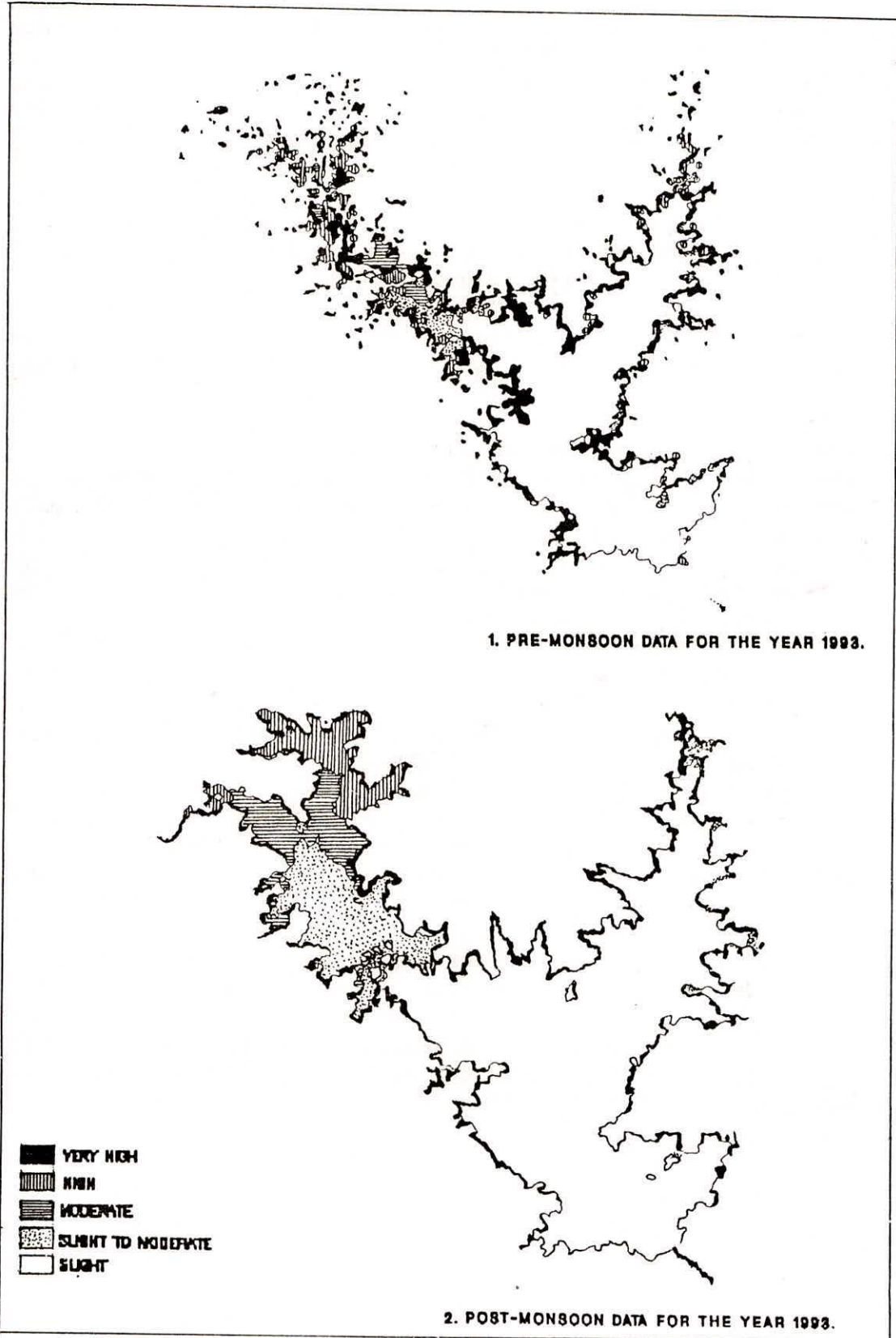
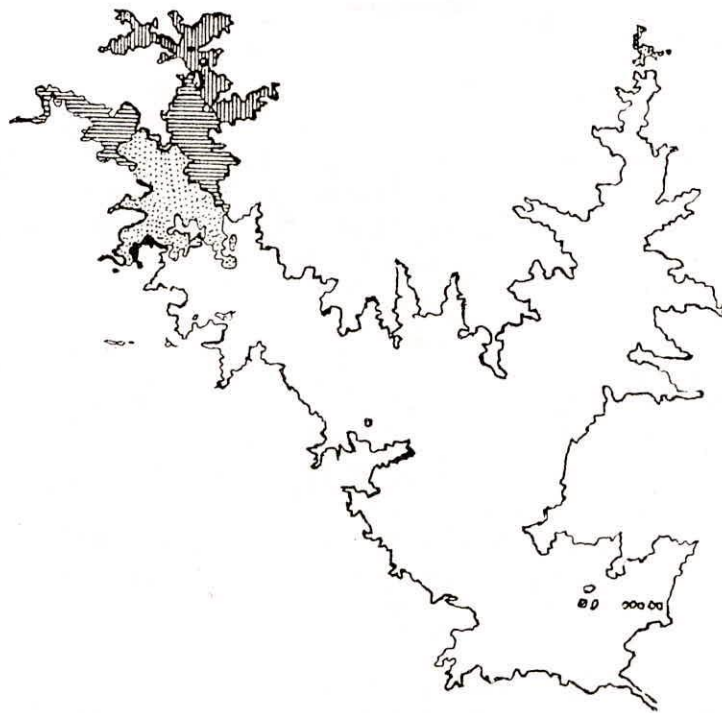
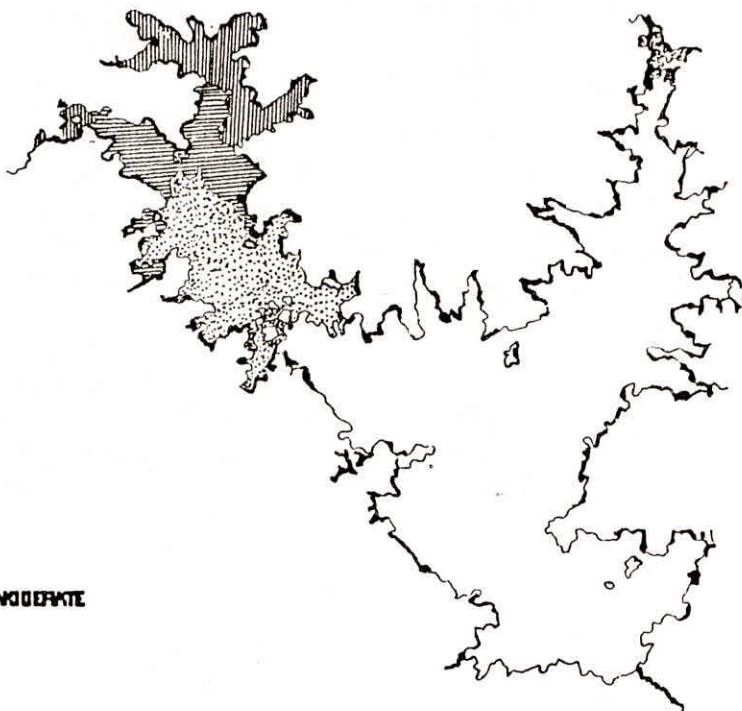


FIG. 9 : SEASONAL SEDIMENT DISTRIBUTION PATTERN



1. POST-MONSOON DATA FOR THE YEAR 1989.



2. POST-MONSOON DATA FOR THE YEAR 1993.



FIG. 10 : YEARWISE SEDIMENT DISTRIBUTION PATTERN

8. CONCLUSIONS

The following conclusions have been drawn:

1. Multi-temporal, multi-spatial and multi-band satellite data are extremely useful in determining sediment distribution pattern in a reservoir and for mapping variation in different concentration levels of suspended sediment present in water.
2. In the present study, the result indicates very high sediment concentration at the tail end of reservoir, moderate to high at fringes and low at dam sites. It indicates that the deposition of suspended sediment, carried by the flood water, in the reservoir end is due to the change in velocity and hydraulics of sediment flow and its deposition pattern in the Mayurakshi river system. Detailed study is essentially required.
3. There is a drastic change in different concentration levels of sediment load during the years 1989 through 1993. The area slightly free from sediment is reduced during this period and there is an increase in sediment concentration. It is a matter of great concern to the Water Resources Engineers and planners. Extensive study of the study area is required to overcome this problem.
4. The results obtained seems to be very promising & the technique can be applied to similar studies very efficiently. The limitation of remote sensing technique should be taken care of before implementing the study.
5. Field survey, toposheets, related reference materials and other ancillary data are equally important to get an updated map of sediment distribution pattern. If possible, Photometers, transmissometers and Secchi disk should be used to get good results.

REFERENCES

1. Alföldi, T.T. and Jr. J.C. Munday (1978), 'Water Quality Analysis by Digital Chromaticity Mapping of Landsat Data', Chandian Journal of Remote Sensing Vol. 4 Nos. 108-126.
2. Amos, C.L. and T.T. Alföldi (1979), 'The determination of Suspended, Sediment Concentration in a Macrotidal System using Landsat Data' Journal of Sedimentary Petrology, Vol. 49, No.1, 159-173.
3. Bressette, W.E. (1974), 'An Optical Filtering System for Remote Sensing of Phyto plankton and suspended Sediment', Proc. Earth Environmental Resources Conference Philadelphia,
4. Brooks, D.J (1975), 'Landsat Measures of Water Quality', Photogrammetry Engg. of Remote Sensing, Vol. 41, No. 10, pp 1269-1272.
5. Bukata, R.P., J.E. Bruton, J.H. Jerome (1983), 'Use of Chromaticity in Remote Measurements of Water Quality', Remote Sensing of Environment, 13, 162-177.
6. Carpenter, D.J. and S.M. Carpenter, (1983), 'Modeling Inland Water Quality Using Landsat Data', Remote Sensing of Environment 13, 345-352.
7. Chaubey. V.K., (1990), Modelling sediment and dissolved load of Tawa reservoir and river (MP) by Remote Sensing techniques, PhD thesis, JNU, New Delhi.
8. Curran, P.J., J.D. Hansom, S.E. Plummer and M.I. Pedly (1987), 'Multispectral Remote Sensing of Nearshore Suspended Sediments : a Pilot Study', INT. J. Remote Sensing, Vol.8 No. 1, 103-112.
9. Deekshatulu, B.L. and S.T. Chari (1981), 'Application of Remote Sensing Techniques for Water Quality Monitoring', Final Project report NRSA.
10. Dubey O.P and H.C.Bhatia (1983), 'Remote sensing for erosion studies in Tehri reservoir', Proc. of National seminar on remote sensing of water resources, Ahemdabad, Dec. 27,1985.
11. Duffuse H.J. and M.J. Press (1984), 'Note on an extension of the Fraser river Plume', Canadian Journal of Remote Sensing, Vol. 7 No. 134-146.
12. Hovis, W.A. and K.C. Leung (1977), 'Remote Sensing of Ocean Color', Optical Engg. Vol., No.1, 158-166.

13. Johnson, R.W. (1975) 'Quantitative Suspended Sediment Mapping Using Aircraft Remotely Sensed Multispectral Data; Proceeding of NASA Earth Resources Survey Symp., Houston Texas, Vol. 1C.
14. Johnson, R.W. (1978), 'Mapping of Chlorophyll distribution in Coastal Zones; Photogrammetric Engineering & Remote Sensing', Vol. 44, No. 5, pp 617-624.
15. Johnson, R.W. and R.C. Harriss, (1980), 'Remote Sensing of Water Quality and Biological Measurement in Coastal Waters', Photogrammetric Engg. and Remote Sensing, Vol. 46, No. 1, pp 77-85.
16. Khorram S. (1981), 'Use of Ocean Color Scanner Data in Water Quality Mapping; Photogrammetric Engg. & Remote Sensing, Vol. 47, No.5, pp 667-676.
17. Khorram S. and Cheshire H. M (1985). 'Remote Sensing of Water quality in the Neuse River estuary North Carolina. Photogrammetric Eng. and Remote Sensing, LI(3), pp. 329-342.
18. Khorram, S., and Cheshire, H.M., (1985), 'Remote Sensing of water quality in the Neuse river estuary, North Carolina, Photogrammetric Engineering and Remote Sensing 51, 329-341.
19. Klemas V., J.F. Borchardt & W.M. Treasure (1973), 'Suspended Sediment Observations from ERTS-1', Remote Sensing of Environment, No. 2, pp. 205.
20. Klemas V., et al (1974), 'Correlation of Coastal, Water Turbidity and Correlation with ERTS-1 and Skylab Imagery' Proc. 9th International Sym. on Remote Sensing of Environment, Ann. Arbor Michigan, Page 1289.
21. Klemas V., et al (1976), 'Application to Ecological, Geological, and Oceanographic Investigation of Delaware bay', Final Report, NRSA CR-144910.
22. Klooster S.A. and J.P. Scherz (1973), 'Water Quality Determination by photgraphic analysis', Proc. 2nd annual Remote Sensing of Earth Resources Conference Tullahoma Tennessee.
23. Kritikos M. and L. Yorinks (1974) 'Suspended Solids Analysis Using ERTS-A Data; Remote Sensing of Environment, Vol. 3, pp.69-78.
24. Lillensand T. M., F.L. Scarpance and J.P. Clapp (1975), 'Water Quality in Mixing zones;' Photogrammetric Engineering and

Remote Sensing, Vol. 41 (7).

25. Lindell Tommy, Karlsson, Rosengren, Mats and Alfoldi, Tom, (1986), 'A further development of the Chromaticity Technique for Satellite Mapping of the Chromaticity Technique for Satellite Mapping of Suspended Sediment load', Photogrammetric Engineering and Remote Sensing, Vol. 52., No.9, pp. 1521-1529.
26. Lindell, L.T. Steinvall., Johnson, O.M., and Classon, T.H., (1985), Mapping of coastall water turbidity using landsat imagery, Int. J. Remote Sensing 6(5), 629-642.
27. Manu, L. and Robertson, C., (1990). Estimating suspended sediment concentrations from spectral reflectance data, Int. J. Remote Sensing 11(5), 913-920.
28. Manvalan, P., G.L. Rajegowada and M.V. Srinivas (1984)' Capacity evaluation of Ghatprabha reservoir using digital analysis of IRS LISS-II data, Project report NO. B/003/91 RRSSC, Bangalore.
29. McCauley, J.R., (1977). Reservoir water quality monitoring with orbital remote sensors, Ph D thesis, Department of Geology, University of Kansas.
30. Moore, G.K. (1980), "Satellite Remote Sensing of Water Turbidity; Hydrological Sciences Bulletin, Vol. 25, no.4 December, 1980.
31. Muley M.V., Amminedu E., Uday R., Chakraborty M. and Tamilarasan V (1986). Water quality mapping in lakes and reservoirs using multitemporal Landsat imagery, IRS-UP/SAC/WQM/SM/03/86, SAC, Ahmedabad.
32. Murlikrishna I.V (1983), 'Landsat Application to Suspended Sediments Evaluation, Chapter 15 of Remote Sensing Application in Marine Science and Technology,' ed. by Crocknell, A.P.D. Reidel publishing company Boston.
33. Murthy T.V.R., Singh T.S., Palria S. and Muley M.V. (1988). Evaluation of digital enhancement techniques for water quality study in the Chilka lake and Matatila reservoir using Landsat Thematic Mapper data. IRS-UP/SAC/WQM/SN/07/88, SAC, Ahmedabad.
34. Nayak, S.R. (1983), 'Orbital Monitoring of Suspended Sediment in Water Bodies', Proc. of National Symposium on Remote Sensing in Development and Management of Water Resources, Ahmedabad, Oct. 25-27, 1983.

35. Palria S., Singh T.S., Muley M. V., Chakravorty M., Tamilarasan V. and Kawosa M.A, (1987), Water quality mapping in the Dal and Wular lakes of Jammu and Kashmir using Landsat images and aerial photographs, IRS-UP/SAC/WQM/SN/05/87, SAC, Ahmedabad.
36. Rao H.S.S. and H.Mahabaleswara (1990), "Prediction of rate of sedimentation of Tungabhadra reservoir", International Symposium on Water Erosion sediment and resource conservation, Oct. 9-13, 1990, Dehradun.
37. Ramsey, E.W and Jensen. J.R., (1990). The derivation of water volume reflectance from airborne MSS data using in situ water volume reflectance and a combined optimization technique and radiative transfer model, Int. J.Remote Sensing 11(6), 977-998.
38. Rimmer, J.C, Collins M. B. and C.B. pattiaratehi, (1987), 'Mapping of Water Quality Incoastal Waters Using Airborne Thematic Mapper Data', INT.J Remote Sensing Vol.8, No. 1, 85-102.
39. Ritchie, J.C., 1976, 'Remote Sensing of Suspended Sediment in Surface Waters, 'Photogrammetric Engg. and Remote Sensing, Vol. 42, No. 12, pp. 1639-1545.
40. Ritchie J.C. and Cooper C. M., (1988). Suspended sediment concentration estimated from Landsat MSS data, Int. J. Remote Sensing, 9 (3) : 379-387.
41. Ritchie, J.C nd Cooper, C.M., (1988) , Suspended sediment concentrations estimated from Landsat NSS data, Int. J. Remote Sensing 9, 379-387.
42. Rogers R.H., L.E. Reed and V.E. Smith (1975), 'Computer Mapping of Turbidity and Circulation Patterns in Saginaw Bay' Michigan (Lake Huron) from ERTS Data, Proc. ASP Convention, Washington DC., Alberta.
43. Sahai B., et al. (1987). Application of remote sensing techniques for watershed characterisation in a part of the Ukai catchment. SAC/RSA-RSAG/SN/02/87. SAC, Ahmedabad.
44. Scarpace F.L. et al (1974), 'Lake Classification Using ERTS Imagery, Proc. Symp. on Remote Sensing and Photo interpretation Comm. G ISP Banff, Alberta.
45. Scherz J.P. (1975), 'Classifying and Monitoring Water Quality by use of Satellite Imagery; Proc. International Conference on Environmental Sensing and Assessment, Los Vegas Nevada,

24 p.

46. Schiebe F.R. J.A. Harrison, J.C.Ritche (1992), "Remote sensing of suspended sediments: the lake chicot, Arkansas Project vol. NO. 13, No.8, 1992.
47. Strandberg C H (1966), 'Water Quality Analysis,' Photogrammetry Engineering, Vol. 32, pp. 234-248.
48. Weeks A.J.H, Simpson (1991), " The measurement of suspended particulate concentrations from remotely sensed data, IJRS vol. 12, No. 4, 1991.
49. Williamson A.N., and W. E. Grabeau (1973), 'Sediment Concentration Mapping in tidal, estuaries; proceedings 3rd earth resources technology satellite 1, symposium vol. 1, Section B pp 1347-1386.
50. Weishlatt E.A. et al. (1973). Classification of turbidity level in Texas marine Coastal Zone. Proceeding of Conference on Machine Processing of Remotely Sensed Data, LARS, Purdue University Oct. 1973, pp. 3A-42 to 3A-59.
51. Yarger H.L., et al (1973), 'Quantitative Water Quality with ERTS-1' Proc. 3rd ERTS-1 Symposium, Vol. 1, Section B., pp 1637-1651.
52. Yarger H.L. et al (1974), Quantitative Water Quality with ERTS-1; Third ERTS-1, Symp., pp. 1637-1651.
53. Yarger H.L., McCauly J.R., James G.W., Magnuson L.M. and Richard G. (1974). Water turbidity detection using ERTS-1 imagery, Proc. of 3rd ERTS-1 Symposium, Washington DC, pp. 651-660.

DIRECTOR

DR. S.M. SETH

HEAD & COORDINATOR

DR. K.K.S. BHATIA

STUDY GROUP

RAMAKAR JHA
MANOHAR ARORA

ASSISTANCE

A.K. SIVADAS
M.B. SANTOSH

